4-7-2011

Wavelet-Based Analysis of Neutron-Induced Photon Spectral Data

Bruce Kessler
Western Kentucky University, bruce.kessler@wku.edu

Alexander Barzilov
Western Kentucky University, alexander.barzilov@wku.edu

Phillip Womble
Western Kentucky University, phillip.womble@wku.edu

2012

Wavelet-Based Analysis of Neutron-Induced Photon Spectral Data

Alexander Barzilov, *Western Kentucky University*
Bruce Kessler
Phillip Womble, *Western Kentucky University*

Wavelet-Based Analysis of Neutron-Induced Photon Spectral Data

Alexander Barzilov, Bruce Kessler, and Phillip Womble

1906 College Heights Blvd., Bowling Green, Kentucky 42101
alexander.barzilov@wku.edu, bruce.kessler@wku.edu, and phillip.womble@wku.edu

Neutron-based methods of non-destructive interrogation of objects for the purpose of their characterization are well-established techniques, employed in the field of bulk material analysis, contraband detection, unexploded ordnance, etc. The characteristic γ-rays produced in nuclear reactions initiated by neutrons in the volume of the irradiated object (inelastic neutron scattering, thermal neutron capture, and activation) are used for the elemental identification. In many real-world applications, an automated spectral analysis is needed, and many algorithms are used for that purpose. The Applied Physics Institute at Western Kentucky University has recently started to employ a mathematical spectrum analysis technique based on wavelets that simultaneously provides quick, accurate, and objective analysis of γ-ray spectra.

This paper will provide a brief overview of wavelets and multiwavelets, and of the wavelet-based analysis algorithm. Examples will be given using neutron-induced photon spectra measured using high resolution and low resolution detectors.

I. INTRODUCTION

Neutron-based analysis methods are an important tool for bulk material analysis[1]. The pulsed neutron technique is an excellent choice to rapidly determine bulk elemental content of a sample in a non-destructive and non-intrusive manner[2]. Pulsed neutron systems are used in industry for on-line analysis of coal[3], cement[4], and metal alloys. Security applications include neutron-based detection of chemical and explosive threats[2] in cargo containers and vehicles, in humanitarian demining, confirmation of unexploded ordinance (UXO), etc.

Neutrons are highly penetrating particles; the typical range is several feet into materials commonly utilized in industry and commerce. As a result of nuclear reactions involving the isotopes contained in the object under scrutiny, the γ-rays are emitted with characteristic and distinct energies. They act like "fingerprints" of these isotopes. Emitted photons are highly penetrating as well. For example, energy of γ-rays emitted from nuclear reactions on nuclei of carbon, oxygen, and nitrogen isotopes is in the range from 4 MeV to 11 MeV. By counting the number of γ-rays emitted with a specific energy, one can deduce the amount of the chemical element that is present in the analyzed sample.

The neutron-based system consists of the source of neutrons, γ-ray detector(s), and associated hardware and software. In our experiments, we used accelerator-based fusion neutron sources - portable neutron deuterium-tritium (d-T) neutron generators. The general scheme of the neutron-based system is shown in Fig. 1.

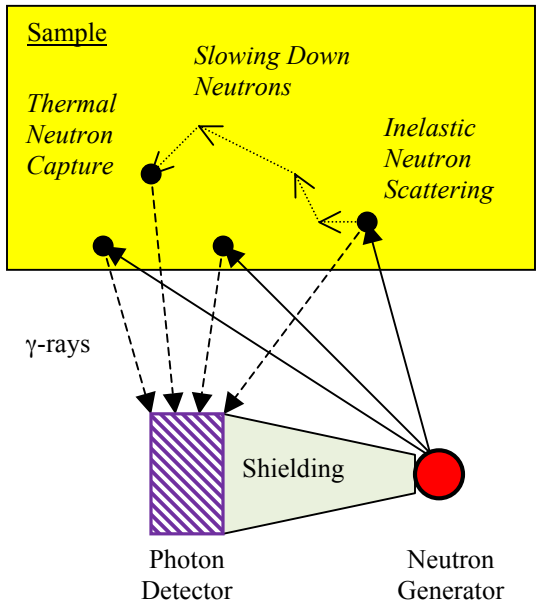

Fig. 1. Neutron elemental analysis scheme.

Pulsed mode of neutron source operation allows simultaneous and separate detection of fingerprint γ-rays from inelastic neutron scattering and thermal neutron capture reactions. It operates as follows. The pulsed d-T generator emits 14-MeV neutrons at 10-kHz frequency with the duty factor of 10%, thus producing the 10 μs-long pulses with the 90 μs-long silence period between pulses. The prompt γ-rays emitted in (n, n'γ) reactions

induced in the sample by fast neutrons are measured by the photon detector in coincidence with the logic signal provided by the neutron generator system. The time delay is utilized in order to take into account the electronic processing time. In between the source pulses, neutrons are slowing down in collisions with low-Z nuclei within the sample and surrounding materials; specific photons from (n, γ) thermal neutron capture reactions are measured in anticoincidence with the generator logic signal. As a result, two separate γ-ray spectra are collected and analyzed for the presence of specific peaks representing isotopes of chemical elements of interest. Intensities of these peaks corresponding to the number of particular nuclei in the sample are used to classify interrogated object based on these elemental characteristics. The γ-rays of the resulting reactions of the elements of interest (H, C, N, O) are of relatively high energy and thus not easily attenuated. Furthermore, since we are measuring the relative intensities of these reactions within a given sample, corrections for the fast and thermal neutron fluences are not necessary. The separation of spectral signatures from different nuclear reactions in this Pulsed Fast Thermal Neutron Analysis (PFTNA)[1,2] provides less complicated spectrum thus allowing the use of low resolution γ-ray detectors.

At the Applied Physics Institute (API) of Western Kentucky University (WKU), the neutron based systems such PELAN[5] (Pulsed ELemental Analysis with Neutrons) and NELIS[6] (Neutron ELemental Inspection System) were developed. PELAN is a man-portable multipurpose neutron probe with a single γ-ray detector. NELIS is based on similar principle but it contains the set of photon detectors for scanning of cargo pallets. Both systems employ a d-T pulsed generator as the neutron source, and BGO scintillation detectors for γ-ray detection. PELAN has been extensively tested in field conditions in UXO and explosive detection applications, chemical weapons detection, and narcotics detection[7,8,9,10]. Similar systems were developed by other groups using NaI(TI) and HPGe detectors: INL vehicle scanner[11], Purdue CarScreen system[12], and several systems by Rapiscan[13].

Neutron based methods generally require a skilled analyst to interpret the γ-ray spectral data collected, and to classify the interrogated object using the elemental parameters extracted from the spectral data. An automatic spectral analysis algorithm for the classification of objects is required for real-world applications where access to nuclear spectroscopy expertise is limited. A wavelet-based algorithm that automatically interprets the spectral data and makes a classification of the substance has been developed to address this need. The algorithm has been experimentally tested at the API at WKU using a laboratory prototype system consisting of a d-T pulsed neutron generator and a γ-ray detector. Both high-resolution semiconductor germanium detectors and lower-resolution scintillation detectors have been used to collect data to test the developed algorithm.

II. WAVELET BASICS

Wavelets and multiresolution analyses are a relatively new tool in the analysis of signals, introduced in the 1970's and formalized during the late 20th century[14]. The main idea is that instead of merely analyzing the frequencies necessary to build a signal, as in the discrete Fourier transform, we look at the signal at different resolutions and keep the error as we go from one approximation to a smoother approximation. This provides not only the information on the high-frequency variations in a signal, but also an indication of the location of where the variation takes place. Wavelets also can ignore large-scale background distortions in spectra, which are predominantly captured in the lowest resolution approximation space instead of the wavelet spaces, making the analysis useful in situations where the background noise varies widely.

II.A. Scaling Functions and Wavelets

A scaling function is a function ϕ that satisfies the dilation equation

$$\phi(x) = \sqrt{2}\sum_{n\in Z} c_n \phi(2x-n) \qquad (1)$$

for some sequence of scalars c_n. When we define linear spaces

$$V_j = \text{clos}_{l^2}\text{span}\left\{\phi\left(2^{-j}\cdot - n\right):\ n\in Z\right\}$$

for integer j, then we have a set of linear spaces, called a multiresolution analysis, that are nested by dilation, such that

$$l^2 \leftarrow \ldots \supset V_{-1} \supset V_0 \supset V_1 \supset \ldots \rightarrow \{0\}$$

where

$$f(x)\in V_j \ \leftrightarrow\ f\left(2^j\right)\in V_{j-1}.$$

The simplest example of a scaling function, and the only single scaling function with any symmetry properties, is the Haar[15] function,

$$\phi(x) = \begin{cases} 1, & \text{for } x\in[0,1) \\ 0 & \text{otherwise} \end{cases},$$

shown in Fig. 2. The Haar function has approximation order 1, meaning that it can reproduce degree 0 polynomials (constants) over a finite interval. The V_0 space generated by the Haar function is the set of square-integrable functions that are piecewise constant on integer knots.

For any given scaling function ϕ and its approximation spaces V_j, we define the wavelet spaces

W_j as the orthogonal complement of V_{j+1} in V_j. We can easily construct a wavelet φ satisfying the dilation equation

$$\varphi(x) = \sqrt{2}\sum_{n\in Z} d_n \phi(2x-n) \tag{2}$$

for some sequence of scalars d_n such that

$$W_j = \text{clos}_{l^2}\text{span}\left\{\varphi\left(2^{-j}\cdot - n\right) :\ n \in Z\right\}$$

for integer j. The wavelet associated with the Haar function is given by

$$\varphi(x) = \begin{cases} 1, \text{ for } x \in \left[0, \frac{1}{2}\right) \\ -1, \text{ for } x \in \left[\frac{1}{2}, 1\right), \\ 0 \text{ otherwise} \end{cases}$$

and is shown in Fig. 2.

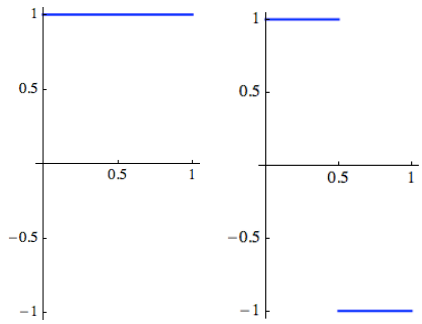

Fig. 2. The Haar scaling function at left, and its associated wavelet at right.

In practice, when analyzing a finite set of uniformly-spaced data $\{y_n\}$, we construct an approximation

$$f(x) = y_n \phi(x-n) \in V_0,$$

which preserves the polynomial order of the data, and find the best approximation into V_1 and W_1. We repeat this process as many times as desired or possible given the number of data points. In general,

$$\begin{aligned} V_0 &= V_1 \oplus W_1 \\ &= (V_2 \oplus W_2) \oplus W_1 \\ &\vdots \\ &= V_k \oplus (W_1 \oplus \ldots \oplus W_k), \end{aligned}$$

so the coefficients of the scaling function and its translates in V_k represent the smoothest approximation of the original data, and the coefficients of the wavelet and its translate in each wavelet space represent the detail lost in each smoothing step. The approximations are found very efficiently if we use an orthogonal scaling function, defined as a scaling function with a finite sequence $\{c_n\}$ in (1) that satisfies the criteria

$$\int_R \phi(x)\phi(x-n)\,dx = \begin{cases} 1, \text{ if } n = 0 \\ 0, \text{ if } n \text{ is a nonzero integer.} \end{cases}$$

With an orthogonal scaling function, best approximations are found by using the $\{c_n\}$ and $\{d_n\}$ in (1) and (2), respectively, as matrix filters that are convolved over the data. The Haar function is an orthogonal scaling function.

II.B. Scaling Vectors and Multiwavelets

Scaling vectors and multiwavelets is a generalization of the structure described in Section II.A. Rather than use a single scaling function ϕ, we use a vector of functions $\Phi = (\phi_1, \ldots, \phi_r)^T$ that satisfy the dilation equation

$$\Phi(x) = \sqrt{2}\sum_{n\in Z} c_n \Phi(2x-n) \tag{3}$$

for some sequence of $r \times r$ matrices c_n. Likewise, each scaling vector will have an associated multiwavelet $\Psi = (\varphi_1, \ldots, \varphi_r)^T$ that satisfies the dilation equation

$$\Psi(x) = \sqrt{2}\sum_{n\in Z} d_n \Phi(2x-n) \tag{4}$$

for a sequence of $r \times r$ matrices d_n. If the scaling vector is orthogonal, with a finite sequence of $\{c_n\}$ and satisfying the criteria

$$\int_R \phi_i(x)\phi_j(x-n)\,dx = \begin{cases} 1, \text{ if } n = 0,\ i = j \\ 0, \text{ if } n \in Z - \{0\},\ i \neq j \end{cases},$$

then best approximations are again easily found using the $\{c_n\}$ and $\{d_n\}$ from (3) and (4), respectively, as matrix filters. The scaling vector used in the algorithm is shown in Fig. 3. The vector has approximation order 4, and the associated approximation space V_0 contains piecewise cubic polynomials on integer knots with a continuity condition and one derivative at each knot[16].

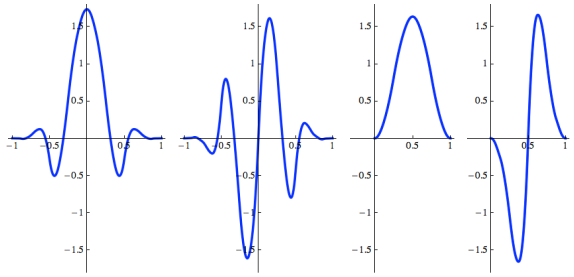

Fig. 3. Scaling vector components used in the algorithm.

There are advantages to using multiwavelets. The scaling vector structure allows for analysis functions that have symmetry and antisymmetry properties, as shown in Fig. 3. The Haar function is the only single scaling function with any symmetry properties[14]. Also, unlike single scaling function constructions, certain types of scaling vector components can be truncated at $x = 0$ to

build boundary functions to handle boundary data without losing the orthogonality of the basis. The major disadvantage is that the process of finding a representation in V_0 for the data set $\{y_n\}$, called prefiltering, is now a nontrivial and possibly noninvertible process[17]. This process has been handled effectively in the algorithm.

III. WAVELET-BASED ALGORITHM

The algorithm used to analyze the data at the API at WKU is the subject of a non-provisional patent pending in the U.S. Patent Office. The author K. is working with a software company to develop commercial software under the name "*Peaklet Analysis*" that implements the algorithm (see www.peakletanalysis.com).

The algorithm takes input from the user prior to the analysis of the spectrum (described in Step 1 below), but then provides a fully automated determination of the relative amounts of the specified elements, and will provide a determination as to closeness of the findings to substances, single or in combinations of two substances, provided by the user.

The steps of the algorithm are provided below. Many of the more proprietary details are necessarily left out of the description.

1) The user inputs the library of peak information for each element that may appear in the data. This information includes the peak center and tolerance for its adjustment, peak widths and tolerance for its adjustment, whether or not the findings for the element is to be reported out, whether or not the peak measurements should be combined with another peak measurement, and relative heights of the peaks (if the user wishes to use the substance match feature).

2) The spectrum data is input, and peak information is automatically adjusted within the given tolerances to match the peaks in the data. Wavelet decompositions are constructed for the spectrum data and for ideal Gaussian peaks according to the adjusted centers and widths.

3) The wavelet decomposition of spectrum data is replaced with a linear combination of the wavelet decompositions of each of the Gaussian peaks, and the spectrum is reconstructed. Nonnegative amounts are found for each peak variable so that the sum of the squares of the differences between the sampled values of the original spectrum and the reconstructed spectrum is minimized.

4) (Optional.) The vector of n variable amounts found in step 3) may then be compared to a library of search compounds input by the user, by finding the angle in n-space between our result and vectors in the library. If $n \geq 3$, then we may find the combination of two substances in the library that minimizes the angle between the "plane" of combinations of the substances and the results from step 3).

IV. EXAMPLES

The neutron generator's trigger signal is used for coincidence measurements. It allows simultaneous detection of fingerprint γ-rays induced in the object by source neutrons. Fig. 4 shows a schematic diagram of the data acquisition system. The photons induced in neutron inelastic scattering nuclear reactions during the neutron pulse (coincident with the "high" status of the trigger signal) are stored in one spectral histogram, and γ-rays emitted in thermal neutron capture nuclear reactions between the neutron pulses ("low" status of the trigger signal) are stored in another spectral storage. Fig. 5 shows the experimental set-up for data collection at the API at WKU.

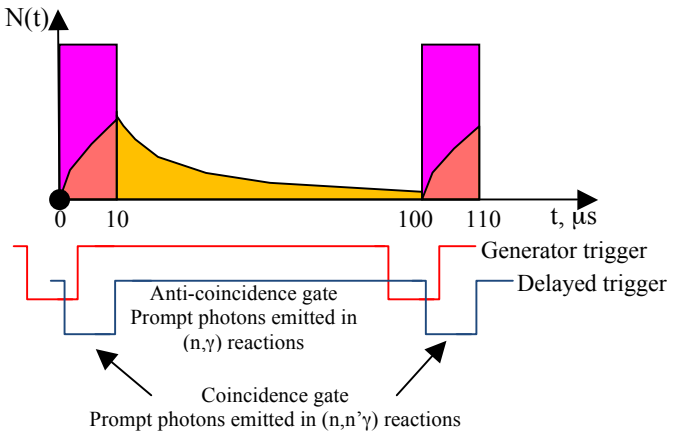

Fig. 4. Scheme of data acquisition system.

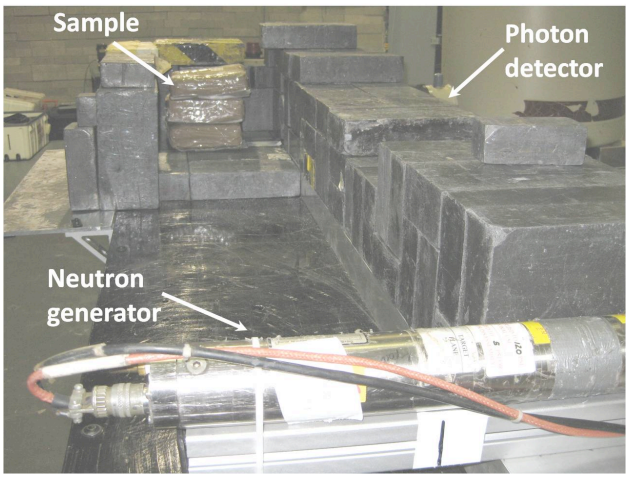

Fig. 5. Experimental setup for wavelet-based algorithm testing.

IV.A. Example 1

The first example is the (n,n'γ) prompt γ-ray spectrum collected from a 2 kg sample of urea irradiated over 10 minutes from 10 cm away with a single HPGe detector, shown in Fig. 6, over the energy range in which we were actively searching for peaks, $[677.9, 6136.3]$ keV. In particular, we are searching for nitrogen peaks near 730 keV (N_2) and 1634 keV (N_1), a carbon peak near 4439 keV (C), and oxygen peaks near 6130 and 5618 keV (O_1 and O_2, respectively). The blue graph is the experimental data, while the red graph is the fit of the data found by the *Peaklet Analysis* software. The green graph is the background curve, as determined by the software, that serves as the bottom of the individual peaks. Fig. 7 shows a close-up of the data and the associated curves over the energy range $[677.9, 1700]$ keV. This figure illustrates nicely the background-identifying abilities of the software, as does Fig. 8, showing a close-up of the graphs over the energy range $[1700, 2300]$ keV. Fig. 9 shows the peak fitting for the oxygen peaks, along with other elements that were included in the search, but not reported out to be included in any ratio calculations.

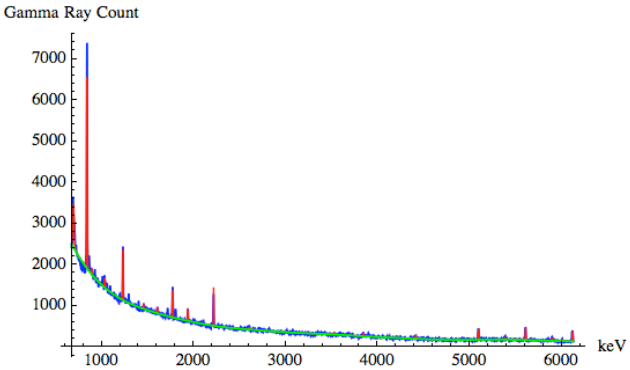

Fig. 6. Coincidental data from a urea sample.

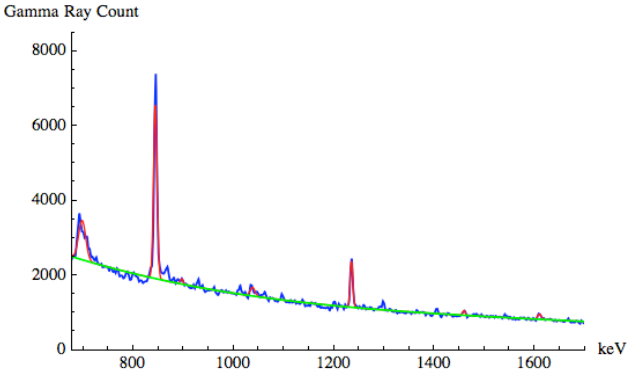

Fig. 7. Close-up of Fig. 6 over $[677.9, 1700]$ keV.

The actual count of γ-rays found for the search elements was

$$(O_1, O_2, C, N_1, N_2) \approx (701, 832, 296, 533, 7524).$$

However, with the relative heights applied to the input peak heights and with the two oxygen peaks combined, the percentage of each search amount was adjusted to

$$(O_1 \ \& \ O_2, C, N_1, N_2) = (15.4, 14.8, 35.6, 34.3).$$

When matching to our library of compounds, we find that this vector is only 3.356 degrees away from our urea vector $(1, 1, 2, 2)$.

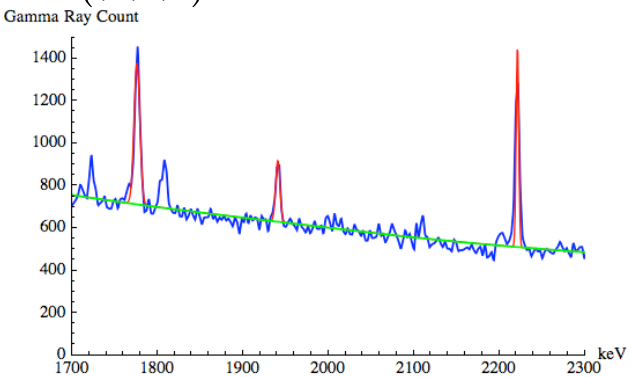

Fig. 8. Close-up of Fig. 6 over $[1700, 2300]$ keV.

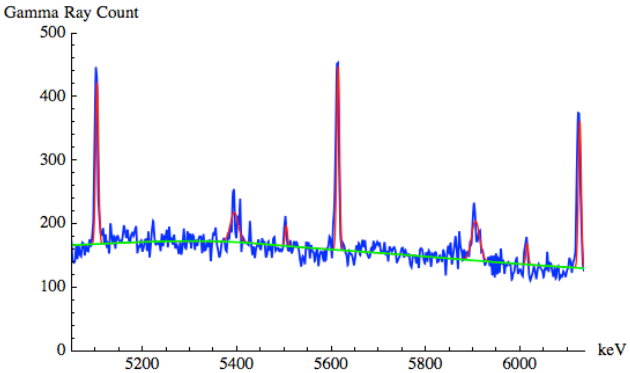

Fig. 9. Close-up of Fig. 6 over $[5050, 6136.3]$ keV.

IV.B. Example 2

In the following example, peaks were placed so that we could illustrate the ability of the software to determine γ-ray counts from overlapping peaks, which may be problematic when using low-resolution γ-ray detectors. In the following example, data peaks were placed at locations 60, 120, 350, and 360, with heights 200, 100, 200, and 150, respectively, with standard deviations 10, 5, 10, and 10, respectively. We have also slightly subtracted a small Gaussian peak of standard deviation 10 away from the location 200, which we also used as a search location. All of this has been placed over a background cubic polynomial, and with Gaussian noise of standard deviation 10 counts added. The result is shown in Fig. 10. Note that the peaks located at 350

and 360 have combined to form what appears to be one single peak.

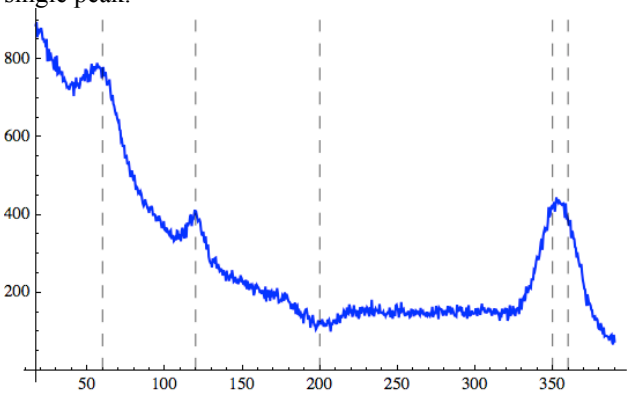

Fig. 10. Low resolution example with overlapping peaks (dashed lines show peak centers).

The software was given the ideal peak locations and the tolerances for recalibration were set to 0 for the 350 and 360 peaks. Thus, we are assuming an accurate calibration of the data. The fit found by the *Peaklet Analysis* software is shown in Fig. 11 in red, with the background curve found by the software shown in green. The percentages of counts found by the software for the peaks at locations $(60,\ 120,\ 200,\ 350,\ 360)$ were

$$(31.27,\ 7.16,\ 0,\ 34.99,\ 26.58),$$

respectively. When compared to the original percentage vector $(33.\overline{3},\ 8.\overline{3},\ 0,\ 33.\overline{3},\ 25)$, we see only a 3.47 degree deviation in the accuracy of the analysis.

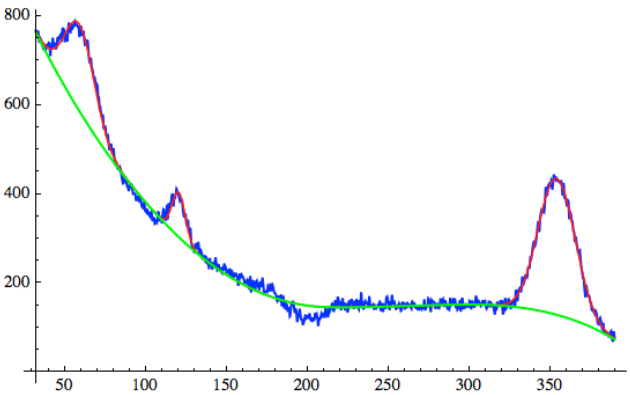

Fig. 11. Fit provided by the software to the spectrum in Fig. 10.

V. CONCLUSION

The wavelet and multiresolution analysis based algorithm has been verified experimentally in the laboratory settings using different test items. It has been shown that the algorithm provides effective analysis of the neutron induced photon spectral data and the classification of materials.

The API researchers are planning to use the developed algorithm to provide automatic analysis of γ-ray spectra in various projects that involve neutron-based material classification. The software that has been developed using the described algorithm is being commercialized and will soon be available for licensing to external users.

ACKNOWLEDGMENTS

The development of the scaling vector used in the algorithm was supported by the Kentucky Science and Technology Corporation (KSTC) through the Kentucky Science and Engineering Foundation (KSEF) Research and Development Excellence grant, KSEF-324-RDE-003. The development of the algorithm was supported by the KSTC through the KSEF Research and Development Excellence grant KSEF-1653-RDE-001. The commercialization of the software implementing the algorithm is supported by the KSTC through the Kentucky Commercialization Fund grant COMMFUND-1280-RFP-011 and by the WKU Research Foundation.

REFERENCES

1. G. Vourvopoulos, P. Womble, "Pulsed Fast Thermal Neutron Analysis: A Technique for Explosives Detection," *Talanta* **54**, pp. 459-468 (2001)
2. P. Womble, G. Vourvopoulos, I. Novikov, and J. Paschal, "Review of Nuclear Methodologies for Explosive Detection," APS Division of Nuclear Physics Meeting, Maui, HI (2001)
3. M. Belbot, G. Vourvopoulos, P. Womble, and J. Paschal, "Elemental On-line Coal Analysis Using Pulsed Neutrons", SPIE Conference "Penetrating Radiation Systems and Applications", SPIE v.3769, p. 168 (1999)
4. P. Womble, J. Paschal, and R. Moore, "Cement Analysis using d+D Neutrons", *NIM B* **241** pp.765-769 (2005)
5. P. Womble, *et al*, "Results of Field Trials for the PELAN System," SPIE Proceedings, v.**4786**, Penetr. Rad. Sys. and Appl. IV, ed. F Doty, pp. 52-57 (2002)
6. A. Barzilov and P. Womble, "NELIS - a Neutron Inspection System for Detection of Illicit Drugs," AIP Conf. Proceedings **680**, pp. 939-942 (2003)
7. D. Holslin, *et al*, "Results of Recent UXO Field Tests at Indian Head with PELAN," Proceedings of UXO/Countermine Forum, Orlando FL (2002)
8. P. Womble, *et al*, "Evaluation of UXO Discrimination Using PELAN," Proceedings of Accelerators in a Nuclear Renaissance, American Nuclear Society (2003)

9. P. Womble, *et al*., "Unexploded Ordnance Discrimination Using Neutrons" First International Meeting on Applied Physics (APHYS-2003), Badajoz, Spain (2003)

10. P. Womble, G. Vourvopoulos, J. Paschal, I. Novikov, and G. Chen, "Optimizing the Signal to Noise Ratio for the PELAN System," *NIM A* **505,** pp.470-473 (2003)

11. E. L. Reber, *et al.,* "Idaho Explosives Detection System", *NIM B* **241**, pp. 738-742 (2005)

12. D. Koltick, S. Mcconchie, and I. Novikov, "A Neutron Based Vehicle Borne Improvised Explosive Device Detection System," in Proc. 8th International Topical Meeting on Nuclear Applications and Utilization of Accelerators, Pocatello (2007)

13. T. Gozani, "The Role of Neutron Based Inspection Technique in the Post 9/11/01 era", *NIM B*, **213**, pp. 460-463 (2004)

14. I. Daubechies, *Ten Lectures on Wavelets*, SIAM (1992)

15. A. Haar, "Zur Theorie der orthogonalen Funktionensysteme", *Mathematische Annalen*, **69**, pp. 331–371 (1910)

16. B. Kessler, "An Orthogonal Scaling Vector Generating a Space of C^1 Cubic Splines Using Macroelements", *J. Concrete Appl. Math. (Special Issue on Wavelets and Applications)*, **4(4)**, pp. 393–413 (2006)

17. D. Hardin and D. Roach, "Multiwavelet prefilters I: Orthogonal prefilters preserving approximation order, $p \leq 2$", *IEEE Trans. Circ. and Sys. II: Anal. and Dig. Sign. Proc.*, **45:8**, pp. 1106–1112 (1998)